

## **Chapter 5**

**Giant Longitudinal negative Maneto-Resistance under out-of-plane magnetic field in  $\text{Bi}_{2-x}\text{Fe}_x\text{Se}_{3-x}\text{S}_x$  Topological Insulators**

## 5.1 INTRODUCTION

The magneto-transport properties in Topological Insulators have attracted lot of attention due to the interesting magneto-resistance behavior in these [69], [73] fact, the topological surface states (TSS) are known to exhibit many promising quantum phenomena associated with the transport studies of topological insulators (TIs) *viz.* weak antilocalization (WAL) [72] and the two dimensional (2D) Shubnikov de-Haas (SdH) oscillation[80] etc. Moreover, positive non-saturating linear magneto-resistance (LMR) is observed in TIs [63].

Recently, magneto transport study of  $\text{Bi}_2\text{Se}_3$  epitaxial layer was executed at low temperature through the study of the angle dependent SdH oscillations which results in the features of both the bulk and surface states simultaneously. Moreover, a strong anisotropic behavior was found in MR, depending on the orientation of current with respect to the magnetic field over a wide range of carrier concentration. A strong negative linear magneto-resistance (NeMR) was also observed while applying the magnetic field parallel to electric one [104].

The recent surge of interest in Dirac Fermions in “3D TI” or “Weyl” semi metals [85] is basically based on their interesting topological properties that features the negative linear magneto-resistance in Weyl semi metal, when the magnetic and electric fields are coaligned. Quantum mechanical phenomena in which number of imbalance chiral fermions exist under an electric field [105] known as axial anomaly, is mainly responsible for NeMR. However, the large negative magneto-resistance (NeMR) under perpendicular magnetic field in Topological insulator has not yet been reported. In a recent study the NeMR has been reported for S doped  $\text{Bi}_2\text{Se}_3$  but the value is very low (<1%) [77]. Moreover, the low NeMR has also been reported in  $\text{TlBi}_{0.15}\text{Sb}_{0.85}\text{Te}_2$  system where at low temperature the resistivity is thermally activated

[100]. However, the origin of the NeMR behavior either for parallel or perpendicular magnetic field is not yet understood.

In this letter, we have reported the magneto-resistance behavior of  $\text{Bi}_{2-x}\text{Fe}_x\text{Se}_{3-x}\text{S}_x$  system. It is observed that with the increase of doping content, magneto-resistance gradually decreases and it reveals giant NeMR at  $\sim 9\%$  of doping. Nevertheless, with further increase of doping concentration, the positive MR reappears. This interesting finding confirms that the observation of NeMR is not present only in Weyl semi metal but also exists in other topological insulators.

## 5.2: Synthesis of Materials

The single crystal  $\text{Bi}_{2-x}\text{Fe}_x\text{Se}_{3-x}\text{S}_x$  [with  $x = 0.06, 0.09$  and  $0.12$ ; we have denoted the doped samples as BiFeS-L, BiFeS-M and BiFeS-H respectively] were grown by melting a stoichiometric mixture with high purity Bi, Se, Fe and S elements which was sealed in evacuated ampoules. We took Fe and S in the equal stoichiometric ratio. The ampoule was heated up to  $900^\circ\text{C}$  at  $200^\circ\text{C}$  per hour and kept for 10 hours and then it was slowly cooled to  $620^\circ\text{C}$  at  $3^\circ\text{C}$  per hour. After that it was cooled down to  $550^\circ\text{C}$  at  $5^\circ\text{C}$  per hour and then it was naturally cooled down to room temperature. Thus obtained crystals were easily cleaved along  $(00l)$  direction. High resolution angle resolved photoemission measurement at 20 meV energy resolution and 0.2 deg angular resolution were performed at the experimental station of angle resolved photoelectron spectroscopy (ARPES) beamline BL-10 at Indus-2 Synchrotron source (India). Single crystal samples were cleaved in-situ to obtain atomically clean surface at room temperature at a base vacuum of  $6 \times 10^{-11}$  mbar. Excitation of monochromatic He-1 line from SPECS (UVS 300) is used to study the ARPES band structure. ARPES data have been recorded with a SPECS Phibos 150 electron energy analyzer. The base vacuum during the measurement was  $7 \times 10^{-11}$  mbar.

## 5.3: RESULT AND DISCUSSION

### 5.3.1: Magneto-Resistance Analysis

The magneto-resistance (MR) of  $\text{Bi}_{2-x}\text{Fe}_x\text{Se}_{3-x}\text{S}_x$  samples as a function of magnetic field at different temperatures is shown in Figure 5.1. Magnetic field was applied along the perpendicular direction of the plane of the samples. We have defined MR as  $[\{\rho(H)-\rho(0)\}/\rho(0)]*100\%$ . It is observed that MR value decreases with doping ( $x=0.06$ ) and with further increase of doping content ( $x=0.09$ ) large negative MR (NeMR) throughout the whole temperature range and magnetic field range is observed. However, if the doping content is further increased positive MR reappears. In the inset we have shown the temperature variation of resistivity under different magnetic fields which supports the magnetic field variation of the MR.

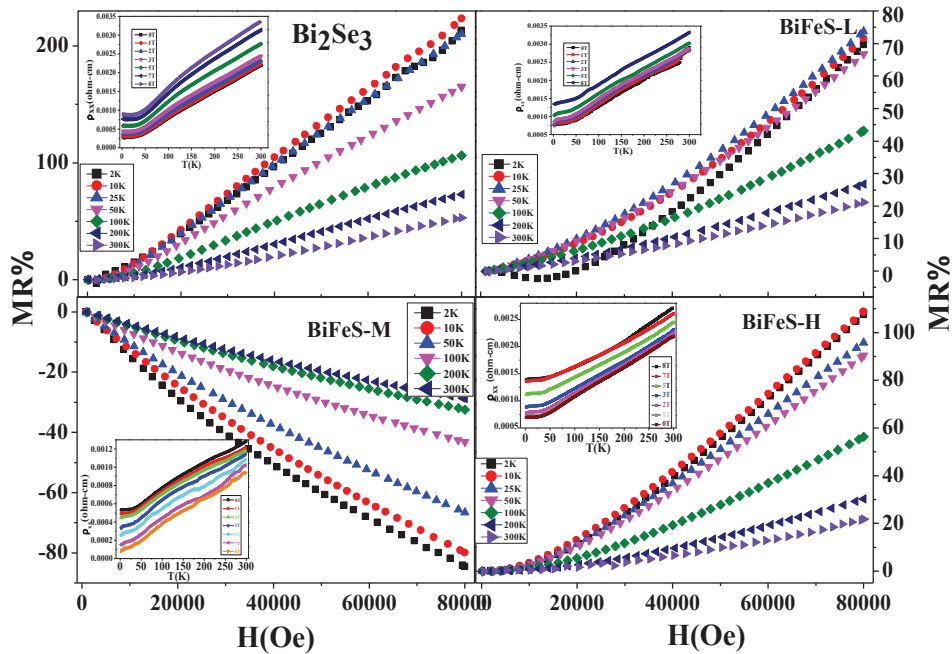


**Figure 5.1:** Magnetic field variation of Magneto-resistance at different temperatures of  $\text{Bi}_2\text{Se}_3$ ,  $\text{BiFeS-L}$ ,  $\text{BiFeS-M}$  and  $\text{BiFeS-H}$ . Inset: Temperature variation of resistivity at different magnetic fields.

Generally, the NLMR in TIs is observed when the applied magnetic field is co-aligned to the electric current and is along the parallel direction to the surface [60]. In the present investigation the NLMR is found when the magnetic field is perpendicular to the surface. Generally, the possible reasons of NLMR are: Kondo effect quenching [91] the existence of ferromagnetic metallic state and the existence of chiral anomaly [93], [94] etc. The chiral anomaly is observed only when the magnetic field is parallel to the electric current. However, in the present investigation the magnetic field is perpendicular to the surface and hence perpendicular to the electric current. Therefore, chiral anomaly is not applicable for the present case. Furthermore, no signature of Kondo effect is observed for the BiFeS-M sample both from the transport and magnetic measurements.

So far, most of the NeMR effects found in 3D TIs are due to the coexistence of weak localization (WL) and weak anti localization effects under low magnetic fields[80].However, in the present investigation for the BiFeS-M sample, NeMR cannot be due to WL effect as the WL induced NeMR saturates at magnetic fields  $\sim 1$  T because of the smaller magnetic length over the phase coherence length in these topological insulators [97], [98]. However, in the present investigation MR is not saturated even at 8T magnetic field. Moreover, the NeMR persists until 300K, which is too high a temperature for WL to exist. Furthermore, in a recent paper [99] it has been proposed that the observed NeMR might be due to the Zeeman splitting which originates due to the spin-orbit coupling on the surface and in the parallel direction to the applied magnetic field. But in the present case the NeMR is observed when the magnetic field is perpendicular to the electric field. Therefore, Zeeman splitting is not the origin of NeMR in our case. Moreover, it has also been observed that charge puddle is also not the origin of the observed NeMR.

### 5.3.2: Magnetic Analysis

In order to further investigate the origin of the observed MR behavior, we have also measured the magnetization with magnetic field at different temperatures (Figure 5.2). It is observed that undoped sample shows diamagnetic behavior but as the doping content increases it shows the ferromagnetic ordering. For BiFeS-M co-doped sample maximum magnetization is observed. As the doping content increases further (BiFeS-H) the magnetization value is decreased. The ferromagnetic behavior is observed even at 300K for the BiFeS-M sample. Therefore, it may be concluded that the negative MR is observed because of the existence of the ferromagnetic ordering. In this case the origin of the magnetic ordering might be the RKKY interaction as has been suggested by Kim et al [77]. From their theoretical calculations, In fact, in the present case the S doping already shifts the Fermi surface to the conduction band [106] and hence the Fe  $3d$  orbital hybridizes with the conduction band. Initially, for low Fe doping the distance between Fe ions is very large and because of the RKKY interaction it shows weak FM ordering [105]. With further increase of Fe content the FM ordering further increases because of the change in  $k_F$  (due to S doping) and also of the change in Fe-Fe distances. But for the highest doped sample, the S already destroys the non-trivial surface state [77] by turning off the spin-orbit coupling [105]. Therefore, there will not be a band inversion anymore and the conduction band without any band inversion cannot work as mediating channels for the magnetic interaction. As a matter of fact, Fe atoms will have independent paramagnetic states without any preferential spin direction and hence, ferromagnetism is decreased.

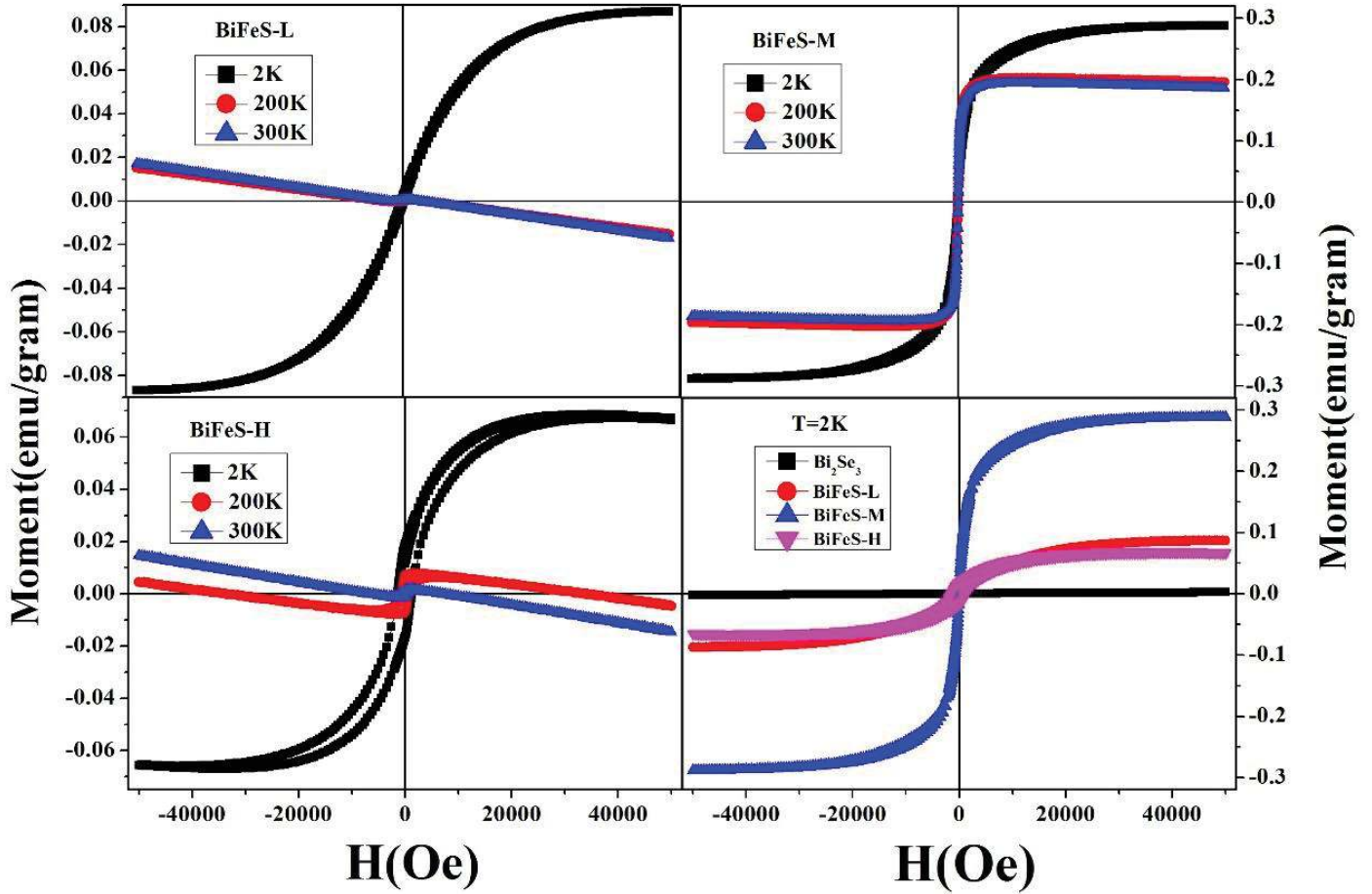
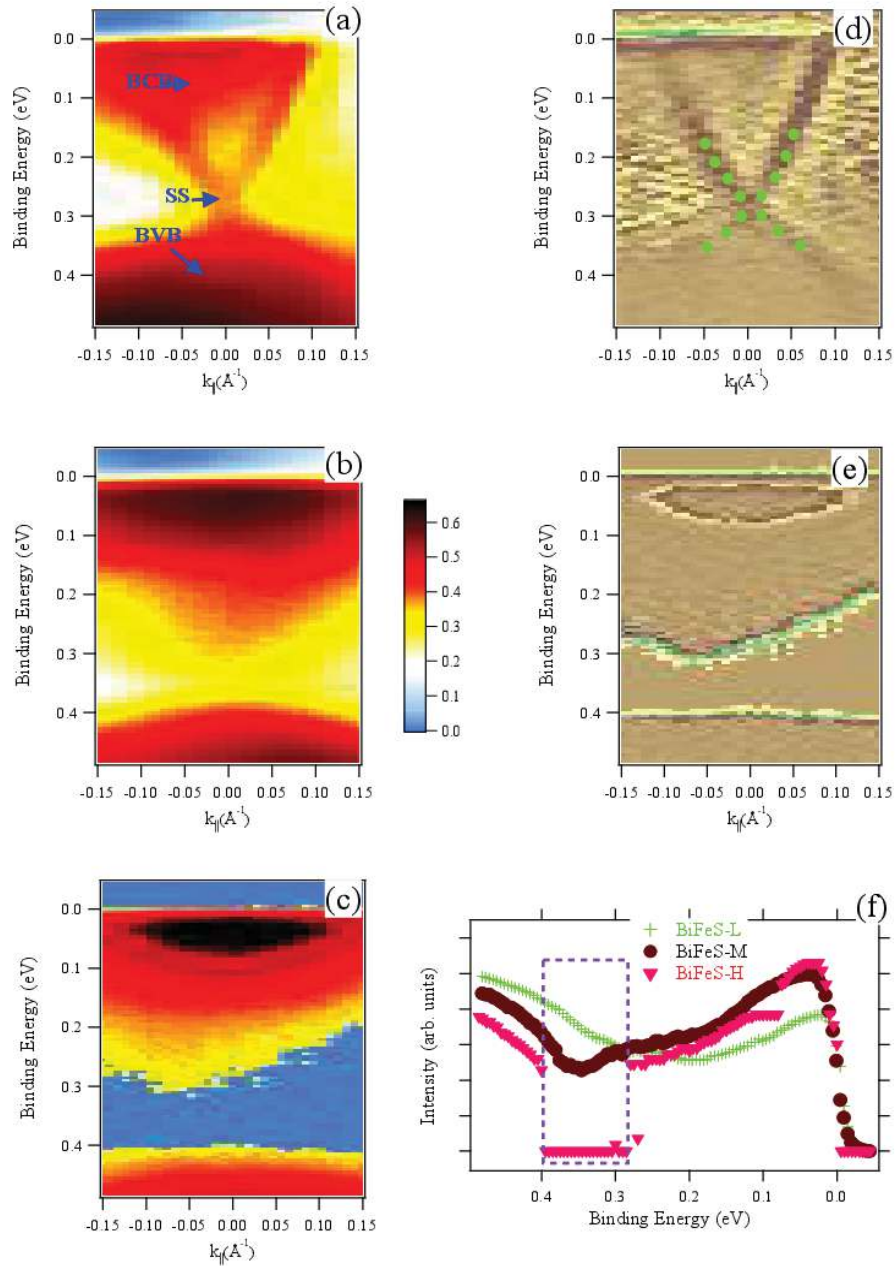


Figure 5.2: Magnetic field variation of magnetization of  $\text{Bi}_2\text{Se}_3$ , BiFeS-L, BiFeS-M and BiFeS-H at different temperatures.

### 5.3.3: Angle Resolved Photoemission Spectroscopy (ARPES)

In order to further investigate we have also measured the ARPES for all the samples. In Figure 5.3 we have shown the ARPES spectra collected for BiFeS-L, BiFeS-M and BiFeS-H. All these spectra are normalized and then plotted using the same color scale for intensity comparison.



**Figure 5.3:** (a), (b) and (c) shows the ARPES spectra of BiFeS-L, BiFeS-M and BiFeS-H respectively collected by photons of energy 21.2 eV. (d) And (e) shows the second derivative of ARPES images for BiFeS-L and BiFeS-H respectively. The green dots in (d) depict the Dirac cone structure. (f) shows the comparison of the EDC's at the  $\Gamma$ -point of the Brillouin zone for all the samples.

For BiFeS-L we observe the bulk conduction band (BCB), the surface state (SS) and the bulk valence band (BVB) for the compound. Such a SS has been observed in  $\text{Bi}_2\text{Se}_3$  previously and is



known to possess the topological protection which arises from the topology of the bulk electronic structure of  $\text{Bi}_2\text{Se}_3$ [16]. These SS possess a linear dispersion (with a Dirac cone structure) as that expected for a massless particle and therefore it comprises of the massless Dirac fermions as opposed to normal fermions [16]. Due to the topological protection the SS is immune to scattering due to non-magnetic disorders introduced on the surface of  $\text{Bi}_2\text{Se}_3$  whereas the introduction of magnetic disorder on the surface results in the loss of the topological protection of the SS due to the breaking of the time reversal symmetry (TRS) thereby opening a gap at the Dirac point [69], [107], [108]. In this study, however, we are attempting to introduce magnetic dopants (i.e. Fe atoms) within the bulk of the  $\text{Bi}_2\text{Se}_3$  matrix and intending to study its effect on the evolution of the SS. So in this case of bulk doping the topology of the bulk electronic structure would be modified and hence it is curious to study its effect on the SS. All the collected ARPES spectra show a portion of the BCB within the occupied region of the ARPES image due to the *n*-type doping of the  $\text{Bi}_2\text{Se}_3$  matrix arising out of the intrinsic Se vacancies within it [109] Furthermore the Fe and S co-doping leads to the additional *n*-type doping as is evident from the gradual shift of the bulk bands towards higher binding energies (BE) with doping. The absence of a band gap in the electronic structure of Dirac fermions on the surface of BiFeS-L shows that the doped magnetic Fe atoms in the sample are not yet sufficient to affect the Dirac cone dispersion at the sample surface. In Figures (d) and (e) we show the second derivative maps of the ARPES intensity (for BiFeS-L and BiFeS-H respectively) which emphasize the electronic bands within an ARPES image. Accordingly, the Dirac cone structure of the Dirac fermions is emphasized in BiFeS-L; however for BiFeS-H the Dirac cone is not visible. Instead, the contours that we observe in case of BiFeS-H arise due to the peripheries of the high intensity regions of its ARPES spectra which in fact correspond to its bulk electronic structure. There is no trace of the

Dirac cone in BiFeS-H as is the case in BiFeS-L. The loss of intensity close to the Dirac point is clearly evident from Figure 5.3(f) where we show the energy distribution curves (EDC) at the  $\Gamma$ -point of the Brillouin zone extracted from Figures 5.3(a), (b) and (c). A comparison between them clearly shows that the ARPES intensity around the region close to the Dirac point (inside the dashed rectangle) reduces as we increase the doping. In BiFeS-H the intensity is negligible and hence there the gap has been fully opened up. We thus conclude the absence of SS and thereby the Dirac fermions in the case of high doping. This is not at all surprising since we are doping magnetic atoms not just at the surface of  $\text{Bi}_2\text{Se}_3$  but right in the bulk in which case we are tampering with the topology of its bulk electronic structure upon which the very existence of the topologically protected SS rests. Thus with the increase in the doping concentration above that of BiFeS-L we observe the absence of the Dirac dispersion and hence we conclude that the non-trivial topology of the bulk electronic structure of  $\text{Bi}_2\text{Se}_3$  matrix has been destroyed. This corroborates well with the SdH oscillations discussed below where the contribution to those oscillations arising from the Dirac fermions is absent. Thus from ARPES studies we conclude that the bulk contribution to the electronic properties of the compound increases with doping which is also consistent with the magnetotransport results.

#### **5.3.4: SdH oscillations and Landau-level fan diagram**

In order to further support the ARPES results we have also shown the fast Fourier transforms (FFTs) of the quantum oscillation (inset Figure 5.4). For undoped and low doped samples we can distinguish the bulk state (lowest frequency peak) and surface states (higher frequency peaks). For the higher doped samples several peaks are observed too. Among these the peaks, those having low widths and low intensities might arise due to the background or due to the contribution of channels of lower mobility. For BiFeS-H, it is observed that the prominent peaks

at higher frequencies are harmonics of the peak at the lowest frequency. Therefore, it is clear that in high doped samples the bulk contribution to the magnetotransport is dominant. The Landau-level fan diagram (Landau index vs.  $1/B$ ,  $B$  being the magnetic field) of all the samples (shown in Figure 5.4) shows an intercept at  $\sim 0.47$  for the undoped and  $\sim 0.41$  for the lowest doped

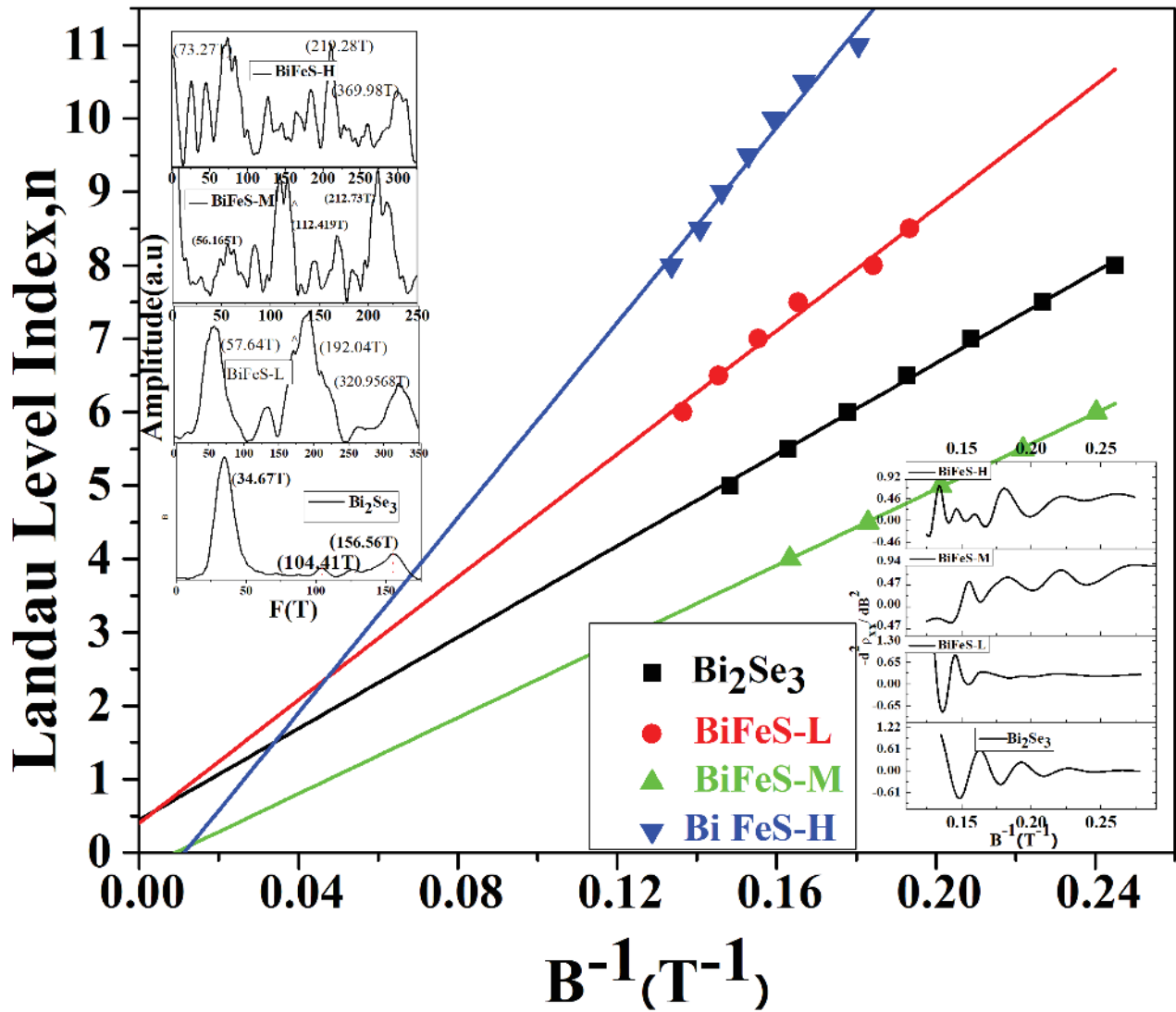


**Figure 5.4:** Landau level index (obtained from MR quantum oscillations) as a function of inverse magnetic field of  $Bi_2Se_3$ ,  $BiFeS-L$ ,  $BiFeS-M$  and  $BiFeS-H$ . Inset (right): Quantum oscillation obtained from magnetic field dependence MR data. Inset (left): First Fourier transform of quantum oscillations.

samples which indicates that the Dirac fermions (with additional Berry phase  $\pi$ ) dominate the transport properties in them. It is found that as the doping content increases the deviation

of the intercept from 0.5 also increases (and becomes close to zero) revealing that in the transport properties the contribution of the Dirac fermion decreases, while the contribution of the normal fermion increases. This also clearly indicates that the bulk conduction gradually dominates over surface conduction with doping and finally for BiFeS-H sample no signature of non-trivial surface state is observed. Therefore, the magneto-transport property is completely consistent with the ARPES study

It is clear from both the ARPES and magneto-transport studies that with increase of doping content the Fermi energy moves into the conduction band. In fact, this happens because of the S doping. This has already been established by us in our previous study [77]. It is observed that increase of S content gradually decreases the MR and at some doping concentration it becomes negative [77]. But value of the negative MR is very low (<1%). Moreover, it has already been reported that Fe doping in TI induces FM ordering [110], [111] But the ordering temperature is very low (<25K). In the present investigation the FM ordering is observed even at 300K. Previously some controversial results were reported about the gap opening of the surface Dirac band with Fe doping in topological insulator. In some paper [108], [111] the gap opening has been reported whereas in some other reports from the ARPES studies [110], [112], it has been claimed that no gap is opened with magnetic ion doping. In fact, the null results are consistent with the report by Kim et [105] where it has been suggested that the positions of the Fermi level moves far from the Dirac point when Fe is doped inducing ferromagnetism without opening the gap. As a matter of fact, the bulk doping of magnetic ions is more effective than the surface doping for controlling the topological characters of those systems. As has been shown in the present investigation from the magnetic, magneto-transport and ARPES studies that for low Fe doping the band gap is not opened yet but FM is induced clearly indicating the bulk doping.

However, the gapped surface state can be realized by bulk doping of magnetic ions [77][131]. We observe in our case also when doping content is increased surface gap is opened. It is obvious that with increase of FM ordering the negative MR enhances and finally for highest doped sample positive MR reappears because of the decrease of ferromagnetism as has been discussed above. The positive linear MR is also observed in non-topological  $\text{Bi}_{1-x}\text{Sb}_x$  material [113]. It is also obvious from the above discussion that the large FM ordering is the simultaneous effect of both Fe and S and this FM ordering is the origin of negative MR. In fact, it is well known that Ferromagnets show a negative MR which arises from the suppression of electron-magnon scattering when a high field opens a gap in the magnon [114], [115] This effect is enhanced with the increase of temperature, as there are then more magnons to suppress. In this case also, NeMR persists upto room temperature as FM ordering exists even at room temperature although the magnetization value decreases as compared to low temperature (due to thermal agitation).

## 5.7: CONCLUSION

In summary, with the increase of doping concentration in  $\text{Bi}_{2-x}\text{Fe}_x\text{Se}_{3-x}\text{S}_x$  MR gradually decreases and for  $x=0.09$  it shows giant negative MR even at room temperature. The negative MR is observed when the system is in the FM state. The origin of FM ordering is attributed to the RKKY interaction. At large doping ( $>9\%$ ) the non-trivial surface state is completely destroyed which in effect destroys the spin-orbit coupling. As a matter fact, the conduction band cannot hybridized with the Fe  $3d$  orbitals as the conduction band is no more inverted and the Fe  $3d$  orbitals will not have any particular orientation. This is the reason of the reappearance of positive MR with larger doping. The ARPES data indicates that above a critical doping concentration ( $x>0.09$ ) the non-trivial bulk state is completely destroyed. Thus we have shown

the loss of the bulk topology of the  $\text{Bi}_2\text{Se}_3$  upon high bulk doping and the interesting MR evolution across the doping which will be useful in technology.